Robotica (2009) volume 27, pp. 321–330. © 2008 Cambridge University Press
doi:10.1017/S0263574708004724 Printed in the United Kingdom

Using optimization to create self-stable human-like running

Katja Mombaur

Interdisciplinary Center for Scientific Computing (IWR), University of Heidelberg, Im Neuenheimer Feld 368, 69120 Heidelberg, Germany.
E-mail: kmombaur@uni-hd.de

(Received in Final Form: April 28, 2008. First published online: June 13, 2008)

SUMMARY
This paper demonstrates how numerical optimization techniques can efficiently be used to create self-stable running motions for a human-like robot model. Exploitation of self-stability is considered to be a crucial factor for biological running and might be the key for success to make bipedal and humanoid robots run in the future. We investigate a two-dimensional simulation model of running with nine bodies (trunk, thighs, shanks, feet, and arms) powered by external moments at all internal joints. Using efficient optimal control techniques and stability optimization, we were able to determine model parameters and actuator inputs that lead to fully open-loop stable running motions.

KEYWORDS: Bipeds; Control of robotic systems; Design; Robot dynamics; Biomimetic robots.

1. Introduction

1.1. Stability control of walking and running in robotics and biomechanics

The past few decades have seen a remarkable development in the field of humanoid robots producing robots that can walk, climb stairs, avoid obstacles, and even lift-off the ground for very short periods of time. Famous examples are Asimo (Honda[15,33]), HRP-2 (Kawada/AIST[18]), Johnnie (TU Munich[11,22]), QRIO (Sony[36]), or Toyota's Partner Robots.[37] But despite this technological progress, there is still a big gap between humanoid robots and their biological counterparts in terms of speed (6 km/h vs. 36 km/h) and efficiency, and it will take many more years, until we will see a robot running as fast and as elegantly as a human.

Stability control of fast motions in general, and running in particular, is still a big technological issue, even though technical signal processing can be faster than neural signal transmission in biology. Most contemporary humanoid robots are still based on conventional robotics control concepts using rigid components and high-gain controllers which are very suitable to satisfy the accurate path following demands of industrial robotics, but seem to be less adequate to bring running motion speeds up to a biological level since the online computational effort for stabilization is too high.

Stability is the property of a system to recover from perturbations of its state. Running in nature is characterized by a high level of self-stability, i.e., the property to automatically recover from perturbations, just by the inherent properties of the mechanical or musculoskeletal system. Brown and Loeb[3] used the term "preflex" to describe such an intrinsic reaction to a perturbance with zero delay. During the biological learning process, walking and running motions evolve in such a way that they harmonically fit to the kinematic and dynamic properties of the walking systems and that the natural stability properties of the system are exploited. Self-stabilizing properties of the muscular actuators also play an important role in biology.[14,21,38] Self-stability is the property that allows animals and humans to run at very high speeds with a relatively low burden on the online control system. Addressing the issue of self-stability therefore seems to be the key to success in making humanoid and other bipedal robots faster.

In order to enhance the stability of humanoid robots, as much intelligence and knowledge as possible should be put into the choice of design parameters and open-loop actuator inputs of a robot. This approach is taken by many researchers of the passive-dynamic walking community, starting with the early research of McGeer.[23,24] From these purely mechanical devices with no actuators walking down inclined slopes, focus has now shifted to actuated mechanisms with some feedback control (see, e.g., Collins et al.[8]). Pratt[32] and Buehler[4] also have built robots that use a combination of natural stabilization and feedback control. Wisse and co-workers in Delft have assembled a remarkable series of passive-dynamic and actuated robots of increasing complexity and with a high level of self-stability[43–45] the tuning of which was mainly based on years of practical robot building and experience.

1.2. Contribution of this paper: generation of open-loop stable running for a human-like robot model using optimization

The contribution of this paper is to look at the problem of tuning the stability properties of a robot model from a more theoretical perspective: it will be shown that using mathematical models and efficient optimization techniques, it is possible to significantly enhance the natural stability properties of a humanoid robot. We present combinations of model parameters and actuation inputs for a human-like running robot such that the resulting running motion is fully open-loop stable.

From a robotics point of view, two different questions can be raised:

https://doi.org/10.1017/S0263574708004724 Published online by Cambridge University Press

1. For a given robot design, which actuator inputs lead to self-stable motions?
2. If the robot design is not yet fully determined, which combination of design parameters and actuation inputs leads to self-stable motions?

Since usually there is at least some freedom in a robot design, and since experience with passive-dynamic walkers has shown how much can be achieved just by parameter modifications, we prefer to address question 2 and will focus on this scenario in this paper. However, if one prefers to explore question 1 in a given situation, this could equally be done by the approach presented in this paper.

This research builds on a series of previous publications of producing, for several simpler robotic models, a variety of open-loop stable motions such as walking,[7,26] running,[29] somersaults,[28] and flip-flops.[25] In this paper, we treat a model of significantly increased complexity: we optimize, for the first time, the stability of a model with torso, arms, and actuated feet. Optimizing parameters and inputs at the same time was only possible due to a new approach to stability optimization modifying all free variables in one optimization loop. The two-level approach used for previous publications only allowed to tune parameters and not controls with respect to stability.

The robot model consists of nine segments and describes human-like sprinting in the sagittal plane. The model has been developed in the thesis,[34] and we have used it before to produce natural looking human-like running based on energy-related optimization criteria.[35] The solutions in that paper were however open-loop unstable, and the availability of appropriate stabilizing feedback control systems had to be assumed. Here, we use stability optimization to produce open-loop stable solutions for a slightly modified runner model. As we will see below, stability is a much more difficult optimization objective than energy and most other common criteria, since it implies the necessity for higher-order derivatives of the trajectories and generally exhibits nondifferentiabilities in the objective function.

We would like to stress the fact that the focus of this paper is stabilization in robotics and not in biomechanics. Even though anthropometric parameters have been used as an example set of starting parameters, this model cannot be used to explain stability of real human running, since one important part is missing in the model: muscle actuators play an important role in biomechanical motion, as mentioned above, and would definitely have to be included in the model in order to attempt an explanation of biomechanical stabilization of running. It is to be expected that optimal motions for a biomechanical model and a robot model would be quite different.

1.3. Review of stability measures

In order to facilitate the discussion of stability of the running model, this section gives a brief overview of different stability measures used in walking robotics. For a longer comparison see, e.g., ref. [31].

Stability of a gait implies that the walking or running system does not fall and that it is able to recover from perturbations. Open-loop stability or self-stability means that this recovery occurs automatically without any feedback implying that the system inputs are not modified at all.

In our study, we only consider strictly periodic motions which are the most basic form of running that should be mastered before more serious perturbations, uneven terrain, and obstacles are taken into account. A stable gait thus represents a periodic limit cycle of the system.

If gaits are regarded from the limit cycle perspective, the most straightforward stability criterion to apply follows the mathematical definition of stability in the sense of Lyapunov's first method (compare, e.g., refs. [9, 16]): a T-periodic solution of a T-periodic non-autonomous system

$$\dot{x}(t) = f(t, x(t)) \text{ with } f(t, \cdot) = f(t + T, \cdot) \qquad (1)$$

is asymptotically stable if all eigenvalues of the monodromy matrix $X(T) = \frac{\mathrm{d}x(T)}{\mathrm{d}x(0)}$ are inside the unit circle

$$|\lambda_i(X(T))| < 1. \qquad (2)$$

It is this eigenvalue criterion that we use to generate open-loop stable motions by means of optimization. This criterion has been applied to gaits by various authors (e.g., Cheng and Lin [5], Coleman [6], Goswami et al. [13], Hurmuzlu [17], and McGeer [23]), who used it to analyze the stability of a given motion, but not in optimization.

In the field of humanoid robots, stability definitions based on the concept of the zero moment point (ZMP), the center of pressure (CoP), or the foot rotation indicator (FRI) play important roles. The ZMP and the CoP[39] define the point where the resulting moment of the ground reaction forces about the horizontal axes lying in the ground vanishes. ZMP and CoP are equivalent, but while the CoP is computed based on ground reaction forces, the ZMP is generally defined using accelerations of the segments. In order to produce stable gaits, ZMP/CoP control algorithms generally aim at keeping this point within the polygon of support, and the distance of the ZMP to the nearest edge of the support polygon is seen as a stability margin. However, this ZMP condition is neither necessary nor sufficient for stable walking. The FRI point[12] is defined as the point where—for a given robot state and acceleration—the resulting ground reaction force would have to be located in order to keep the foot fixed. This is equivalent to the ZMP for a ZMP lying inside the polygon of support, but it can also define negative stability margins. What is important to note for the purpose of this paper is that all ZMP-related concepts are made for flat-foot contact and are not directly applicable to motions with flight phases and pointwise contact phases.

Pratt and Tedrake[31] present velocity-based stability margins that can also be applied to irregular gaits, and can easily be measured and computed, but are restricted to fast walking with at least one foot in ground contact at any time.

Other criteria that seem to have some relationship to stability are concerned with minimizing the total angular momentum about the center of mass (c.o.m.)[30] or the widely used minimization of jerk known to produce smooth motions, or of other derivatives of the c.o.m. trajectory to produce viability.[42] Some of these criteria might present an alternative

https://doi.org/10.1017/S0263574708004724 Published online by Cambridge University Press

to classical Lyapunov stability and will be investigated for the bipedal running model in a future publication.

1.4. Outline of paper

The remaining sections of this paper are organized as follows: Section 2 describes the model of the two-dimensional humanoid running robot. Section 3 outlines the formulation and solution of optimal control problems for the generation of optimal periodic gaits—with and without inclusion of stability criteria on the problem. Section 4 presents self-stable running motions for the humanoid model that have been computed using the presented optimization approach. In Section 5, we finally formulate some conclusions and future research directions.

2. Model of a Two-Dimensional Humanoid Runner

For the investigations in this paper, we use a model of a two-dimensional humanoid runner with nine segments (one torso and two thighs, shanks, feet, and arms). The model is a slightly modified version of the two-dimensional model presented in ref. [35] to which we refer for more details. It describes human-like forefoot running in the sagittal plane which does not include flat-foot ground contact at any instant, but point-like contact with the ball of foot.

Running motions consist of multiple motion phases, where each phase is characterized by different sets of governing equations and possibly different degrees of freedom (DOF). We only consider strictly periodic and symmetric running gaits, such that the order of phases is *a priori* known (single-foot contact phases alternating with flight phases) and can be prescribed in the model. In addition, due to the symmetry, the periodic cycle investigated can be reduced to one step with a subsequent shift of sides. Impacts at touchdown are assumed to be fully inelastic, and no sliding between foot and ground occurs. Arms are modeled as one segment each, with both elbow angles fixed to 100° during the whole running motion. We also use the simplifying assumption that the ankle angle is fixed to 90° during the step in which it does not encounter ground contact. This results in a model with 10 DOF for one step and 11 DOF for the overall running motion involving left and right steps. In the model, we use the coordinates

$$\begin{aligned} q^T := (&y_{\text{pelvis}}, z_{\text{pelvis}}, \phi_{\text{trunk}}, \phi_{(\text{stance hip})}, \phi_{(\text{stance knee})}, \\ &\phi_{(\text{stance ankle})}, \phi_{(\text{swing hip})}, \phi_{(\text{swing knee})}, \phi_{(\text{arm (stance side)})}, \\ &\phi_{(\text{arm (swing side)})}) \end{aligned}$$

and corresponding velocities $v = \dot{q}$. The first three components of q describe position and orientation of the pelvis and the remaining components indicate relative interior angles at the joints. This same set of coordinates is used for the description of both flight and contact phase representing in the first case a set of minimal coordinates, and redundant coordinates in the latter case.

The equations of motion during flight phase are formulated as a set of ordinary differential equations of the following general form:

$$M(q, p)\ddot{q} + N(q, \dot{q}, p)\dot{q} = F(q, \dot{q}, p, \mathcal{M}), \tag{3}$$

where M is the symmetric positive-definite mass matrix of the system, vector N combines all nonlinear effects, and F denotes the sum of all external forces acting on the multibody system. F depends on gravity, motor torques $\mathcal{M}$ and other applied active forces, moments and forces of spring-damper elements (with spring constants k_i, offset angles $\Delta\phi_i$, and damper constants b_i)

$$F_{\text{sd},i}(q_i, \dot{q}_i) := k_i(q_i - \Delta\phi_i) - b_i\dot{q}_i, \quad i = 2, \ldots, 9, \tag{4}$$

drag (with the simplifying assumption that only drag on the trunk in horizontal direction plays a role, using air density ρ_{air}, drag coefficient c_w, trunk cross section A_{tr}, and forward speed $\dot{q}_0$)

$$F_{\text{drag}} \approx F_{\text{drag, trunk, } y} = -c_w \frac{\rho_{\text{air}}}{2} A_{\text{tr}} \dot{q}_0^2, \tag{5}$$

etc. For the model used in this paper, the terms M and N which both are too complicated to be derived by hand have been established using the automatic model generator of the software package HuMAnS.[41]

During single leg contact phase, additional constraints of form $g(q) = 0$ describing the point-like contact of the ball of foot with the ground have to be taken into account, which results in a system of differential algebraic equations (DAE) of index 3.

We formulate this model in the equivalent form of an index-1 DAE with invariants

$$\dot{q} = v \tag{6}$$

$$\dot{v} = a \tag{7}$$

$$\begin{pmatrix} M & G^T \\ G & 0 \end{pmatrix} \begin{pmatrix} a \\ \lambda \end{pmatrix} = \begin{pmatrix} -N + F \\ \gamma \end{pmatrix} \tag{8}$$

$$g_{\text{pos}} = g(q(t), p) = 0 \tag{9}$$

$$g_{\text{vel}} = G(q(t), p) \cdot \dot{q}(t) = 0, \tag{10}$$

with acceleration vector $a := \ddot{q}$, and the vector of Lagrange multipliers λ. G is the derivative matrix of the position constraints, $G = (\partial g/\partial q)$, and γ the right-hand side of the acceleration constraints, $\gamma = ((\partial G/\partial q)\,\dot{q})\,\dot{q}$. (9) and (10) are the invariants on position and velocity level. The fact that ground contact only represents a unilateral constraint (i.e., ground can only push against the foot but not pull) is taken into account in the optimization by formulating an inequality constraint on the Lagrange multiplier associated with the normal contact force.

The model formulation uses a set of free model parameters p. These parameters include characteristic data of each segment (segment length, relative c.o.m. location, mass, and moment of inertia for planar motion), and parameters of spring-damper elements in all joints.

Phase changes between flight phase and single-leg contact phase do not occur at fixed times, but depend on the position variables of the robot, which can be expressed by zeroes of switching functions of the following general form:

$$s(q(\tau_s), v(\tau_s), p) = 0. \tag{11}$$

https://doi.org/10.1017/S0263574708004724 Published online by Cambridge University Press

Touchdown occurs when the lowest point of a foot reaches zero height, and lift-off is characterized by a vanishing vertical contact force (which corresponds to a vanishing Lagrange multiplier in Eq. (8)).

The lift-off event is smooth, but the impact at touchdown results in velocity discontinuities $\Delta v = v_+ - v_-$ of all components of the system, which can be computed solving the following system of equations (using the same matrices as in (8), see ref. [40]):

$$\begin{pmatrix} M & G^T \\ G & 0 \end{pmatrix} \begin{pmatrix} v_+ \\ \Lambda \end{pmatrix} = \begin{pmatrix} M v_- \\ 0 \end{pmatrix}. \tag{12}$$

An artificial discontinuity is introduced in the model at the end of the cycle to describe the swap of variables describing left and right half of the robot.

Periodicity constraints are imposed in the model on all velocity variables v and a reduced set of position variables q_{red} eliminating the coordinate describing the forward running direction of the robot

$$\begin{pmatrix} q_{\text{red}}(T) \\ v(T) \end{pmatrix} = \begin{pmatrix} q_{\text{red}}(0) \\ v(0) \end{pmatrix}. \tag{13}$$

T is the step time of the running cycle which, along with the individual phase times, is a free variable of the model.

3. Generation of Open-Loop Stable Periodic Running Motions

Simulation-based optimization, or optimal control, is a useful tool to generate motions, since in contrast to approaches based on pure simulation it allows to leave both the trajectory and the force and torque inputs free and to determine them simultaneously.

The problem of generating an optimal periodic gait can be formulated as multiphase optimal control problem

$$\min_{x(\cdot),u(\cdot),p,\tau} \quad \int_0^T \phi(x(t), u(t), p)\, \mathrm{d}t + \Phi(T, x(T), p) \tag{14}$$

$$\text{s.t.} \quad \dot{x}(t) = f_j(t, x(t), u(t), p) \quad \text{for} \quad t \in [\tau_{j-1}, \tau_j], \quad j = 1, \ldots, n_{\text{ph}}, \ \tau_0 = 0, \tau_{n_{\text{ph}}} = T \tag{15}$$

$$x(\tau_j^+) = x(\tau_j^-)) + J(\tau_j^-) \quad \text{for} \quad j = 1, \ldots, n_{\text{ph}} \tag{16}$$

$$g_j(t, x(t), u(t), p) \geq 0 \quad \text{for} \quad t \in [\tau_{j-1}, \tau_j] \tag{17}$$

$$r_{\text{eq}}(x(0), \ldots, x(T), p) = 0 \tag{18}$$

$$r_{\text{ineq}}(x(0), \ldots, x(T), p) \geq 0. \tag{19}$$

This formulation uses free variables of different types:

- $x(t)$ is the vector of state variables and summarizes the positions and velocity variables of the robot model $x^T = (q^T, v^T)$.
- $u(t)$ is the vector of control or input variables of the system. For the model used in this paper, u corresponds to the motor torques $\mathcal{M}_i$ applied at all internal joints.
- p is the vector of model parameters described in Section 2.
- τ is the vector of phase switching times which also determines the cycle time $T = \tau_{n_{\text{ph}}}$; here we have $\tau^T = (\tau_{\text{flight}}, \tau_{\text{contact}})$.

Eq. (14) describes the objective function in a very general form. Different sets of constraints are considered in the optimal control problem:

- Eqs. (15) and (16) stand for appropriate ODE/DAE models of the hybrid dynamics of the robot with multiple continuous phases and discrete phases, as described in Section 2
- Continuous inequality constraints of form (17) on all optimization variables, including simple lower and upper bounds on controls, states, and parameters, but also more complex relations between several variables
- Pointwise equality and inequality constraints on all variables, (18) and (19), including conditions for single points (start point/end point/phase switching conditions) as well as relationships between several distinct points, such as periodicity constraints.

Possible candidates for objective functions of form (14) are, e.g., functions related to energy consumption, efficiency, speed, step frequency, and stride length.

The situation however gets more complicated if stability is to be taken into account, as done in this paper. Asymptotic open-loop stability is the property of a solution to persist, even under small perturbations, with all perturbed solutions eventually converging back to the original unperturbed solution.

This stability property of a solution is directly related to the sensitivities, i.e., derivatives of its end values with respect to its initial values. In addition to the quantities used in (14), an objective function describing stability therefore also requires

$$X(T) = \frac{\mathrm{d}\, x(T)}{\mathrm{d}\, x(0)}, \tag{20}$$

which is the monodromy matrix associated with the solution (also termed Jacobian of the Poincaré map).

As described in Section 1.3, asymptotic stability in the sense of Lyapunov requires that for all eigenvalues of $X(T)$, we have $|\lambda_i(X(T)| < 1$, i.e., for the spectral radius $\rho := |\lambda_i(X(T))|_{\max} < 1$. Note that this stability criterion is also valid for hybrid multiphase systems, as we have shown in ref. [27]. This results in using the spectral radius as objective function for stability optimization

$$\min \rho(X(T)). \tag{21}$$

If not all entries of x are periodic, the nonperiodic directions have to be eliminated by projection prior to usage in the above criterion. The same has to be done in the case of autonomous systems (i.e., systems without input variable) with the direction associated with the invariant eigenvalue of one that always exists in this case.

Other than the spectral radius, possible choices for objective functions are induced norms on the monodromy

https://doi.org/10.1017/S0263574708004724 Published online by Cambridge University Press

matrix, such as the 1- or ∞-norm or the singular value, which all are upper bounds on the spectral radius and therefore represent stricter measures of stability.

In any case, first-order derivative information of the trajectory is required, and the resulting optimal control problem formulation for stability computations becomes

$$\min_{x(\cdot),X(\cdot),u(\cdot),p,\tau} \int_0^T \phi(x(t),u(t),p)\,\mathrm{d}t + \Phi(T,x(T),X(T),p) \tag{22}$$

$$\text{s.t.} \quad \dot{x}(t) = f_j(t,x(t),u(t),p) \quad \text{for} \quad t \in [\tau_{j-1},\tau_j], \quad j = 1,\ldots,n_{\text{ph}}, \quad \tau_0 = 0, \tau_{n_{\text{ph}}} = T \tag{23}$$

$$x(\tau_j^+) = x(\tau_j^-)) + J(\tau_j^-) \quad \text{for} \quad j = 1,\ldots,n_{\text{ph}} \tag{24}$$

$$\dot{X}(t) = \frac{\partial f_j}{\partial x}(t,x(t),u(t),p)X(t) \quad \text{for} \quad t \in [\tau_{j-1},\tau_j] \quad \text{with} \quad X(0) = I \tag{25}$$

$$X(\tau_j^+) = \left((f_{j+1}(\tau_j^+) - f_j(\tau_j^-) - J_t - J_x f_j(\tau_j^-))\frac{1}{\dot{s}}s_x^T + I + J_x\right)X(\tau_j^-) \quad \text{for} \quad j = 1,\ldots,n_{\text{ph}} \tag{26}$$

$$g_j(t,x(t),u(t),p) \geq 0 \quad \text{for} \quad t \in [\tau_{j-1},\tau_j] \tag{27}$$

$$r_{\text{eq}}(x(0),\ldots,x(T),p) = 0 \tag{28}$$

$$r_{\text{ineq}}(x(0),\ldots,x(T),X(T),p) \geq 0. \tag{29}$$

In addition to the modifications in (22), this formulation includes augmented dynamics in the form of the variational differential equation (25) and the corresponding update formula (26) taking into account that phase switching points would be shifted in time in the presence of perturbations.

Our experience has shown that using only stability as an objective function does not lead to natural and efficient motions. We therefore use either a combination of stability and some energy or efficiency-related measure in the objective function, or formulate stability not as an objective function at all but as a constraint, as indicated by the usage of $X(T)$ in (29), e.g.,

$$\rho(X(T)) \leq c < 1, \qquad \text{e.g., } c = 0.8. \tag{30}$$

For the solution of the above problem, we built upon the optimal control methods based on the direct boundary value problem methods developed by Bock and co-workers (MUSCOD[2,19,20]) and adapted them to handle index-3 DAE. Optimal control problems in the forms given above are infinite-dimensional (since $x(t)$ and $u(t)$ are variables in function space), but can be transformed into finite-dimensional problems by means of discretization. The MUSCOD method uses a direct approach for control discretization, using base functions with local support, such as piecewise constant, linear, or cubic functions. State parameterization is performed by the multiple shooting technique which transforms the original boundary value problem into a set of initial value problems with corresponding continuity and boundary conditions. The same grid is used for both parameterizations (controls and states). The resulting structured nonlinear programming problem is solved by an efficient tailored sequential quadratic programming (SQP) algorithm. It is important to note that this approach still includes a simulation of the full problem dynamics on each of the multiple shooting intervals. This is performed simultaneously to the nonlinear programming solution using fast and reliable integrators also capable of an efficient and accurate computation of trajectory sensitivity information.[1]

The spectral radius criterion, no matter if as optimization criterion or as a constraint, has a serious difficulty: it becomes nondifferentiable, and sometimes even non-Lipschitz at points of multiple maximum eigenvalue. SQP techniques, however, in general require second-order differentiable functions. But our numerical experiments have shown that—despite this violation of theoretical assumptions at certain iterates—the optimal control techniques described above work very well using finite differences for gradient evaluation, even at nondifferentiable points. It delivers much better results in much shorter computation times than our previous two-level optimization methods that took into account the nondifferentiability of the objective function and used a split of variables[27] and derivative-free optimization techniques in the outer loop.

4. Results of Stability Optimization

In this section, we present stability optimization results for the two-dimensional bipedal running model (see Fig. 1). Formulating problem (22)–(29) for the biped results in an optimal control problem with 420 state variables ($= 20 + 20^2$, including the augmented dynamics), 7 control variables, 59 model parameters, and 2 free phase times. We apply a piecewise constant control discretization. Both control and state parameterization are performed on a grid with 16 intervals for the flight phase and 24 intervals for the contact phase. Two transition phases of duration zero are used to describe ground impact after flight phase and switching of left and right half. All constraints discussed in Section 2 are formulated in the optimization problem, along with suitable upper and lower bounds on all optimization variables (states, controls, parameters, and phase times). Among them is a lower bound on the velocity of the pelvis in forward direction (here chosen as 5 m/s) in order to produce a significant forward running motion. The dimensions of the optimal control problem given above after discretization result in a nonlinear programming problem with 18,415 unknown variables, 17,673 equality constraints, and 36,881 inequality constraints.

The following optimization criteria have been applied:

- At first, stability has been optimized, using the eigenvalue criterion given in Eq. (21).

https://doi.org/10.1017/S0263574708004724 Published online by Cambridge University Press

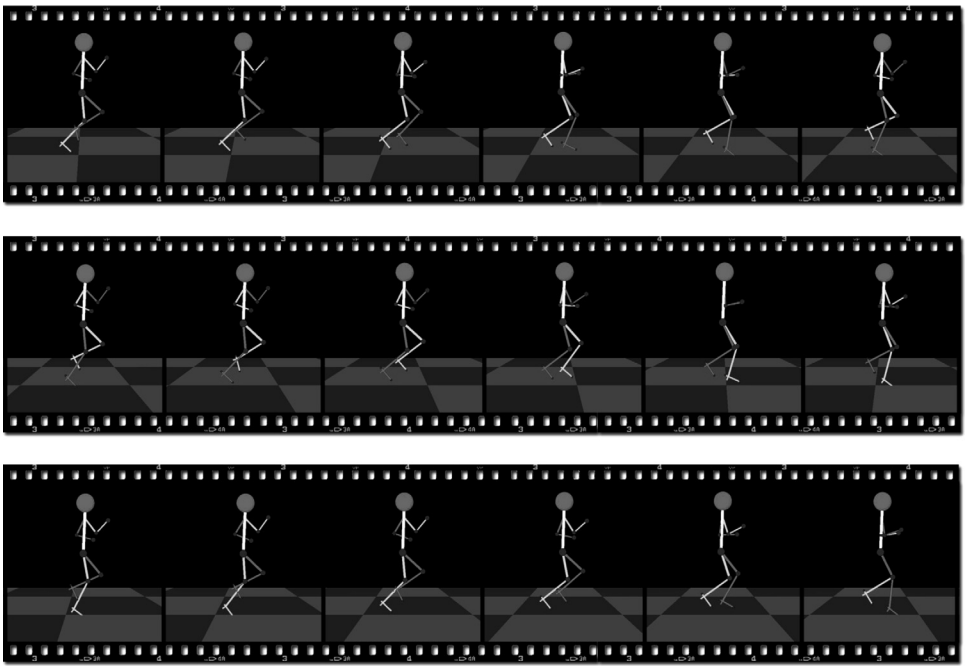


Fig. 1. 2D running motion resulting from stability optimization.

- Second, starting from the solution of the first problem, a minimization of torques squared has been applied

$$\int_0^T u^T u \, \mathrm{d}t \tag{31}$$

which is considered a measure for energy (electrical, not mechanical), while a constraint is imposed on the spectral radius (see Eq. (30) using $c = 0.8$). The purpose of the second step is to make the solution smoother. We have varied input torque histories, state variable trajectories, phase durations as well as all model parameters.

Figure 2 shows the position histories for the resulting open-loop stable solution. It is characterized by a spectral radius of 0.8. The initial values of the positions are

$$\begin{aligned} q(0) = (&0.00, 9.30\mathrm{E}-01, -4.24\mathrm{E}-02, 8.15\mathrm{E}-01, \\ &-1.883, -3.24\mathrm{E}-01, 1.06\mathrm{E}-1, -7.68\mathrm{E}-01, \\ &-5.16\mathrm{E}-01, 7.45\mathrm{E}-01)^T \end{aligned}$$

and of the velocities

$$\begin{aligned} \dot{q}(0) = &(5.324, 5.60\mathrm{E}-01, 2.77\mathrm{E}-01, 1.65\mathrm{E}-01, 4.101, \\ &-2.297, 1.856, -6.607, 1.121, -2.454)^T. \end{aligned}$$

Figure 3 gives the corresponding torque histories. The resulting phase durations are 0.106 s for flight and 0.088 s for contact, i.e. $T = 0.194$ s for a step. The overall step length is $\Delta y = 1.017$ m which corresponds to an average speed of $\bar{v} = \bar{\dot{q}}_0 = 5.24$ m/s. Both state variable and control

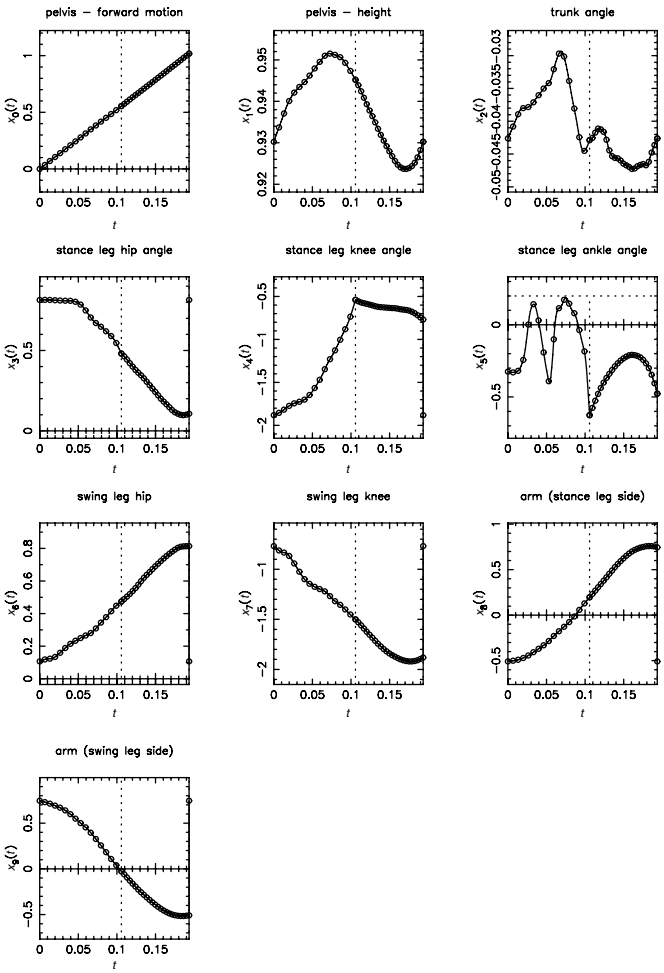


Fig. 2. Position histories for open-loop stable running motion.

https://doi.org/10.1017/S0263574708004724 Published online by Cambridge University Press

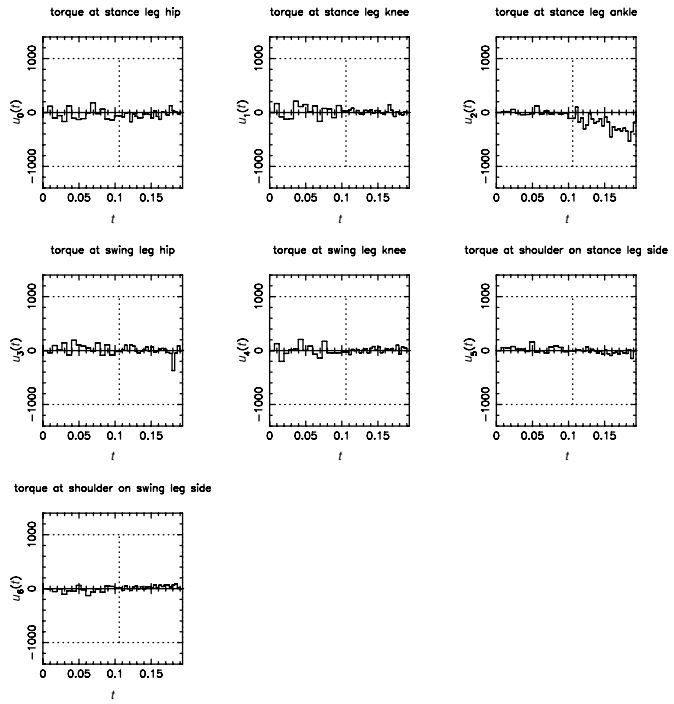


Fig. 3. Torque (control variable) histories for open-loop stable running motion.

variable histories are very different from the corresponding unstable starting solutions. Figure 4 shows a comparison of the starting trajectory and the self-stable solution. The stable solution is characterized by a reduced forward speed, a smaller step length, and a more upright trunk position. The shorter steps result in smaller extremal leg angles at the hip, and thus a more elevated hip position during the whole step. The ankle joint shows a small wiggle which apparently does not influence stability too much but is still undesirable and might be avoided using additional constraints.

The computations show that it is in fact possible to produce open-loop stable running for a human-like model.

We started with human data for segment lengths, masses, and moments of inertia of all bodies. This data has been left free (within bounds) during optimization. In addition, parameters of all spring-damper elements acting at interior joints have been varied. Tables I–V show the development of all model parameters during stability optimization. They indicate start values and final values after optimization and relative change. We give these numbers only for a qualitative assessment of which groups of parameters tend to change about which magnitudes. It is not the exact values of these numbers that matter, especially since it can be assumed that the optimization problems have several local minima.

Since human-like parameters (taken from ref. [10]) have been used for initialization, the segmentation used for parameterization follows that of biomechanical literature and does not directly correspond to the model described in Section 2. As indicated by the lines in Tables I and II, several segments of the biomechanical model are summarized (assuming rigid coupling) to form the bodies of the optimization model of Fig. 5:

- Lower trunk, mid trunk, upper trunk, and head are combined to one single trunk segment.
- Upper arm, forearm, and hand on each side are summarized to form the arms.

Shank, thigh, and foot also appear in the optimization model as separate bodies (with the exception of the swing leg for which shank and foot are fixed to each other).

Table I shows the changes of all segment masses. It is important to note that none of them changes significantly

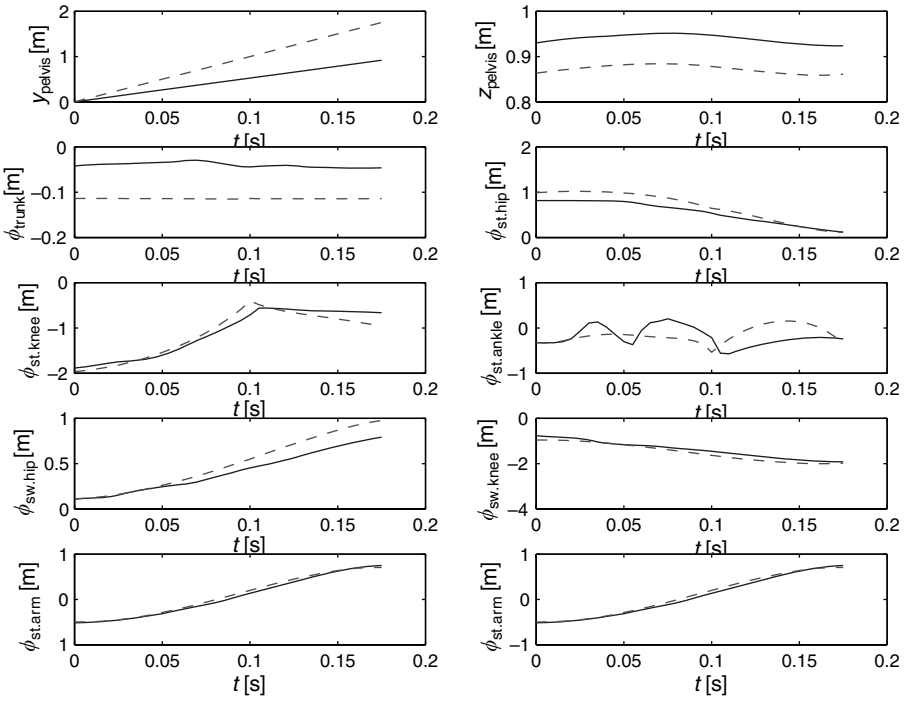


Fig. 4. Comparison of position variable histories of starting trajectory (dashed line) and of open-loop stable solution (solid line).

https://doi.org/10.1017/S0263574708004724 Published online by Cambridge University Press

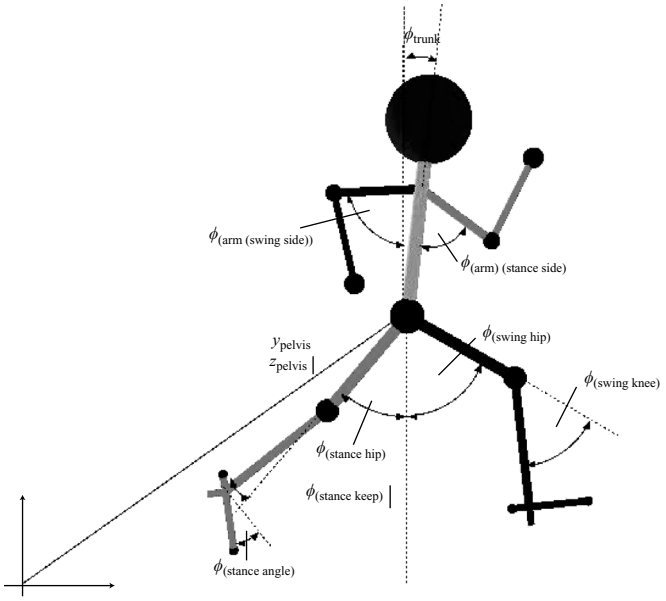


Fig. 5. Coordinates of the two-dimensional humanoid running model.

with maximum changes of 3%. None of the mass parameters reaches its bounds. The same is true for the inertia parameters $I_i = m_i r_{gyr}^2$ shown in Table II which exhibit a maximum change of ≈4%. The overall mass of the model also barely changes (from 73 kg to 73.03 kg).

Tables III and IV show the development of the segment lengths and segment c.o.m. positions measured from the proximal end of the segments. Again, the changes are relatively small (at maximum 4.5% and 3.5%, respectively), and no bounds are attained. The overall height of the model changes from 1.75 m to 1.74 m during optimization.

The last group of parameters considered are those describing the spring-damper elements of form (4) active in each joint. For the leg joints, they were allowed to be different in flight and in contact. The development of these parameters during optimization is shown in Table V. In contrast to all other groups considered above, these model parameters can be subject to significant changes, up to the order of 100%.

Table I. Optimization of model parameters: segment masses.

Segment	Start value (kg)	Optimized value (kg)	Change (%)
Lower trunk	8.150E+00	8.054E+00	−1.17
Mid trunk	1.192E+01	1.189E+01	−0.22
Upper trunk	1.165E+01	1.165E+01	0.02
Head	5.070E+00	5.080E+00	0.20
Thigh	1.034E+01	1.043E+01	0.93
Shank	3.160E+00	3.142E+00	−0.56
Foot	1.000E+00	9.978E-01	−0.22
Upper arm	1.980E+00	1.963E+00	−0.83
Forearm	1.180E+00	1.176E+00	−0.29
Hand	4.450E-01	4.589E-01	3.13

Table II. Optimization of model parameters: segment inertia.

Segment	Start value (kg m^2)	Optimized value (kg m^2)	Change (%)
Lower trunk	9.160E-02	9.555E-02	4.32
Mid trunk	2.960E-01	3.043E-01	2.84
Upper trunk	3.400E-01	3.385E-01	−0.43
Head	6.110E-02	6.018E-02	−1.50
Thigh	5.080E-01	5.177E-01	1.91
Shank	1.570E-01	1.589E-01	1.22
Foot	4.980E-03	5.053E-03	1.48
Upper arm	6.510E-02	6.656E-02	2.26
Forearm	2.440E-02	2.423E-02	−0.66
Hand	3.510E-03	3.340E-03	−4.84

Table III. Optimization of model parameters: segment lengths.

Segment	Start value (m)	Optimized value (m)	Change (%)
Lower trunk	1.457E-01	1.489E-01	2.26
Mid trunk	2.155E-01	2.123E-01	−1.46
Upper trunk	1.707E-01	1.706E-01	0.00
Thigh	4.222E-01	4.099E-01	−2.9
Shank	4.403E-01	4.457E-01	1.24
Dist. heel-ball	1.900E-01	1.956E-01	2.97
Foot	2.100E-01	2.100E-01	0.00
Dist. pelvis-shoulders	5.155E-01	5.386E-01	4.49
Upper arm	2.817E-01	2.771E-01	−1.62
Forearm	2.689E-01	2.729E-01	1.51

Table IV. Optimization of model parameters: segment c.o.m. positions.

Segment	Start value (m)	Optimized value (m)	Change (%)
Lower trunk	5.700E-02	5.668E-02	−0.54
Mid trunk	1.185E-01	1.146E-01	−3.27
Upper trunk	1.195E-01	1.228E-01	2.82
Head	8.200E-02	8.004E-02	−2.39
Thigh	1.730E-01	1.681E-01	−2.82
Shank	1.940E-01	1.946E-01	0.32
Foot	4.800E-02	4.841E-02	0.86
Upper arm	1.630E-01	1.573E-01	−3.46
Forearm	1.230E-01	1.200E-01	−2.40
Hand	6.950E-02	6.909E-02	−0.58

In addition, the parameter describing the drag acting on the runner [see Eq. (5)]

$$F_{\text{drag}} = -d_{\text{drag}} v^2 \text{ with } d_{\text{drag}} = c_w \frac{\rho_{\text{air}}}{2} A \qquad (32)$$

in the order of 0.16 kg/m (resulting from $\rho_{\text{air}} \approx 1.2$ kg/m^3, $c_w \approx 1.0$, and $A \approx 0.27$ m^2) changes from this initial value of 0.16 to 0.155 (−3.4%).

Summing up this analysis of parameter variations, it is important to note for the optimization run investigated we observe the following lucky coincidence: the parameters that would be harder to modify in a design such as masses, inertias, segment lengths, and c.o.m. positions have not been changed much by the optimization, while other parameters

https://doi.org/10.1017/S0263574708004724 Published online by Cambridge University Press

Table V. Optimization of model parameters: spring-damper parameters.

Spring/damper element	Start value (m)	Optimized value (m)	Change (%)
$k_{\text{hip, flight}}$	4.576E-01	7.211E-01	57.57
$b_{\text{hip, flight}}$	4.315E-01	4.774E-01	10.64
$k_{\text{hip, contact}}$	2.890E+00	2.245E+00	−22.32
$b_{\text{hip, contact}}$	2.128E+00	2.092E+00	−1.69
$\Delta\Phi_{\text{hip}}$	1.209E-01	1.204E-01	−0.41
$k_{\text{knee, flight}}$	4.364E-01	5.333E-01	22.19
$b_{\text{knee, flight}}$	1.103E-01	1.079E-01	−2.13
$k_{\text{knee, contact}}$	2.869E+00	2.906E+00	1.31
$b_{\text{knee, contact}}$	1.591E+00	1.640E+00	3.11
$\Delta\Phi_{\text{knee}}$	−2.040E-01	−2.526E-01	23.79
$k_{\text{ankle, flight}}$	1.832E+00	1.990E+00	8.58
$b_{\text{ankle, flight}}$	9.580E-01	9.934E-01	3.70
$k_{\text{ankle, contact}}$	1.707E+00	1.632E+00	−4.40
$b_{\text{ankle, contact}}$	3.141E-02	6.499E-02	106.92
$\Delta\Phi_{\text{ankle}}$	7.851E-02	1.050E-01	33.82
k_{shoulder}	5.000E-01	3.524E-01	−29.51
b_{shoulder}	6.461E-01	6.412E-01	−0.77
$\Delta\Phi_{\text{shoulder}}$	0.000E+00	1.801E-02	–

which might more easily be changed in a design such as spring-damper elements are subject to larger variations. Other computations not presented here have shown that it is even possible to produce open-loop stable motions if the parameter groups of Tables I–IV are fixed, and only spring-damper elements left free.

It is of course not possible to derive a general rule from these computations, but it seems likely that it will be possible to stabilize a variety of humanoid robot designs using some free model parameters and all control and trajectory variables. The most significant stabilization effects come from the variation of the actuator inputs and of the trajectory.

5. Conclusions and Future Research

The results of this paper show that it is possible to produce bipedal human-like running motions that are stable without feedback. This has been achieved for a model with 11 DOF and torque actuators with parallel spring-damper elements at all interior joints. These results are very encouraging for the design of humanoid robots. If correctly applied to a good model of a humanoid robot, the presented stability optimization techniques might be very helpful in the design phase of the robot and in the choice of actuator inputs during operation. As a consequence, the complex task of stability control should be considerably simplified for these robot motions, even in the presence of perturbations, due to the better exploitation of self-stability of the dynamical system.

The research might also be extended in the biomechanical direction: incorporating models of appropriate muscle actuators in the human-like running model might make it possible to explain the stabilizing mechanisms of fast human track running in more detail.

Another possible research direction is the investigation of alternative optimization criteria with possible relation to stability, as discussed in Section 1.3.

Acknowledgments

The research project has been supported by the Postdoc Program of the foundation Landesstiftung Baden-Württemberg and by the German Ministry of Education and Research (BMBF) within the framework "*Bionik – Innovationen aus der Natur*". The work of Gerrit Schultz, who established the model equations of the bipedal robot, is gratefully acknowledged.

References

1. H. G. Bock, "Randwertproblemmethoden zur Parameteridentifizierung in Systemen nichtlinearer Differentialgleichungen," **In**: *Bonner Mathematische Schriften 183* (Universität Bonn, 1987).
2. H. G. Bock and K.-J. Plitt, "A Multiple Shooting Algorithm for Direct Solution of Optimal Control Problems," *Proceedings of the 9th IFAC World Congress*, Budapest, International Federation of Automatic Control (1984) pp. 242–247.
3. I. E. Brown and G. E. Loeb, *Neuro-control of posture and movement*, chapter A reductionist approach to creating and using neuromusculoskeletal models (Springer-Verlag, New York, 2000).
4. M. Buehler, "Dynamic locomotion with one, four and six-legged robots," *J. Rob. Soc. Jpn.* **20**(3), 15–20 (Apr. 2002).
5. M.-Y. Cheng and C.-S. Lin, "Measurement of robustness for biped locomotion using a linearized Poincaré map," *Robotica* **14**, 253–259 (1996).
6. M. J. Coleman, A Stability Study of a Three-Dimensional Passive-Dynamic Model of Human Gait. *Ph.D. Thesis* (Cornell University, Feb. 1998).
7. M. J. Coleman, M. Garcia, K. D. Mombaur and A. Ruina, "Prediction of stable walking for a toy that cannot stand," *Phys. Rev. E* **2** 022901 1–3 (2001).
8. S. H. Collins, A. L. Ruina, R. Tedrake and M. Wisse, "Efficient bipedal robots based on passive-dynamic walkers," *Science* **307**, 1082–1085 (2005).
9. J. Cronin, *Differential Equations—Introduction and Qualitative Theory* (Marcel Dekker, New York, 1994).
10. P. de Leva, "Adjustments to Zatsiorsky-Seluyanov's segment inertia parameters," *J. Biomech.* **9**, 1223–1230 (1996).
11. M. Gienger, K. Löffler and F. Pfeiffer, "Design and realization of Jogging Johnnie," *CISM Courses and Lectures* (2002) pp. 445–452.
12. A. Goswami, "Postural stability of biped robots and the foot rotation indicator (FRI) point," *Int. J. Rob. Res.* **18**(6), 523–533 (1999).
13. A. Goswami, B. Espiau and A. Keramane, "Limit Cycles and Their Stability in a Passive Bipedal Gait," *Proceedings of IEEE International Conference on Robotics and Automation*, Minneapolis (1996) pp. 246–251.
14. H. Wagner and R. Blickhan, "Stabilizing function of sceletal muscles: An analytical investigation," *J. Theor. Biol.* **199**(2), 163–179 (1999).
15. Honda. Honda robots webpage, http://www.honda-robots.com (2007).
16. J. C. Hsu and A. U. Meyer, *Modern Control Principles and Applications* (McGraw-Hill, New York, 1968).
17. Y. Hurmuzlu, "Dynamics of bipedal gait: Part II – Stability analysis of a planar five-link biped," *J. Appl. Mech.* **60**, 337–343 (June 1993).
18. K. Kaneko, F. Kanehiro, S. Kajita, H. Hirukawa, T. Kawasaki, M. Hirata, K. Akachi and T. Isozumi, "Humanoid Robot hrp-2," *Proceedings of ICRA 04*, IEEE RAS (May 2004) pp. 1083–1090.
19. D. B. Leineweber, I. Bauer, H. G. Bock and J. P. Schlöder, "An efficient multiple shooting based reduced SQP strategy for large-scale dynamic process optimization—Part I: Theoretical aspects," *Comput. Chem. Eng.* **27**, 157–166 (2003).

https://doi.org/10.1017/S0263574708004724 Published online by Cambridge University Press

20. D. B. Leineweber, A. Schäfer, H. G. Bock and J. P. Schlöder, "An efficient multiple shooting based reduced SQP strategy for large-scale dynamic process optimization—Part II: Software aspects and applications," *Comput. Chem. Eng.* **27**, 167–174 (2003).
21. G. E. Loeb, "Control Implications of Musculosceletal Mechanics," *Annual International Conference IEEE-EMBS*, Montreal (1995) Vol. 17, pp. 1393–1394.
22. S. Lohmeier, K. Löffler, M. Gienger, H. Ulbrich and F. Pfeiffer, "Computer System and Control of Biped Johnnie," *Proceedings of ICRA 04*, New Orleans IEEE RAS (2004).
23. T. McGeer, "Passive dynamic walking," *Int. J. Rob. Res.* **9**, 62–82 (1990).
24. T. McGeer, "Dynamics and control of bipedal locomotion," *J. Theor. Biol.* **163**, 277–314 (1993).
25. K. D. Mombaur, "Performing Open-Loop Stable Flip-Flops—An Example for Stability Optimization and Robustness Analysis of Fast Periodic Motions," *Fast Motions in Robotics and Biomechanics—Optimization and Feedback Control*, Lecture Notes in Control and Information Science (Springer, Heidelberg, 2006).
26. K. D. Mombaur, H. G. Bock, J. P. Schlöder and R. W. Longman, "Human-Like Actuated Walking that is Asymptotically Stable Without Feedback," *Proceedings of IEEE International Conference on Robotics and Automation*, Seoul, Korea (May 2001) pp. 4128–4133.
27. K. D. Mombaur, H. G. Bock, J. P. Schlöder and R. W. Longman, "Open-loop stable solution of periodic optimal control problems in robotics," *ZAMM—J. Appl. Math. Mech.* **85**(7), 499–515 (July 2005).
28. K. D. Mombaur, H. G. Bock, J. P. Schlöder and R. W. Longman, "Self-stabilizing somersaults," *IEEE Trans. Rob.* **21**(6) (Dec. 2005) pp. 1148–1157.
29. K. D. Mombaur, R. W. Longman, H. G. Bock and J. P. Schlöder, "Open-loop stable running," *Robotica* **23**(01), 21–33 (Jan. 2005).
30. M. Popovic, A. Englehart and H. Herr, "Angular Momentum Primitives for Human Walking: Biomechanics and Control," *Proceedings of the IEEE/RSJ International Conference on Intelligent Robots and Systems*, Sendai, Japan (2004).
31. J. Pratt and R. Tedrake, "Velocity-based stability margins for fast bipedal walking," *Fast Motions in Robotics and Biomechanics—Optimization and Feedback Control*, Lecture Notes in Control and Information Science (Springer, Heidelberg, 2006).
32. J. E. Pratt, Exploiting Inherent Robustness and Natural Dynamics in the Control of Bipedal Walking Robots. *Ph.D. Thesis* (Massachusetts Institute of Technology, 2000).
33. Y. Sakagami, R. Watanabe, C. Aoyama, S. Matsunaga, N. Higaki and K. Fujimura, "The Intelligent ASIMO: System Overview and Integration," *Proceedings of IROS*, IEEE/RSJ (Dec. 2002) Vol. 3, pp. 2478–2483.
34. G. Schultz, Generation of Optimal Human Running Gaits *Master's Thesis* (University of Heidelberg, 2007).
35. G. Schultz and K. Mombaur, "Modeling and optimization of human-like running motions," submitted.
36. Sony, QRIO—World's first running humanoid robot, press release, `http://www.sony.net/SonyInfo/News/Press_Archive/200312/03-060E/` (2003).
37. Toyota, Toyota Partner Robots, `http://www.toyota.co.jp/en/special/robot/` (2007).
38. A. J. van Soest and M. F. Bobbert, "The contribution of muscle properties in the control of explosive movements," *Biol. Cybernet.* **69**, 195–204 (1993).
39. M. Vukobratovic and B. Borovac, "Zero-moment point—Thirty-five years of its life," *Int. J. Humanoid Rob.* **1**(1), 157–173 (2004).
40. P.-B. Wieber, Modélisation et commande d'un robot marcheur anthropomorphe. *Ph.D. Thesis* (Ecole des Mines de Paris, 2000).
41. P.-B. Wieber, "Holonomy and nonholonomy in the dynamics of articulated motion," *Fast Motions in Biomechanics and Robotics—Optimization and Feedback Control* (Springer, Heidelberg, 2006) pp. 411–425.
42. P.-B. Wieber, "Viability and Predictive Control for Safe Locomotion," *Proceedings of JNRR 2007 (Journées Nationales de la Recherche en Robotique)*, Obernai, France (2007).
43. M. Wisse, "Three Additions to Passive Dynamic Walking: Actuation, an Upper Body and 3D Stability," *Proceedings of IEEE/RAS International Conference on Humanoid Robots*, Tsukuba, Japan (2005) pp. 295–300.
44. M. Wisse, C. G. Atkeson and D. K. Kloimwieder, "Dynamic stability of a simple bipedwalking system with swng leg retraction," *Fast Motions in Robotics and Biomechanics—Optimization and Feedback Control*, Lecture Notes in Control and Information Science (Springer, Heidelberg, 2006).
45. M. Wisse and J. van Franzenhuyzen, "Design and Construction of "Mike": A 2D Autonomous Biped Based on Passive Dynamic Walking," *Proceedings of International Conference on Adaptive Motion of Animals and Machines (AMAM)*, Kyoto, Japan (2003).

https://doi.org/10.1017/S0263574708004724 Published online by Cambridge University Press